Materials Research Express

PAPER

Effect of annealing temperature on the properties of Ag doped ZnO thin films

RECEIVED
27 April 2018

REVISED
10 August 2018

ACCEPTED FOR PUBLICATION
17 August 2018

PUBLISHED
31 August 2018

F Lekoui[1,2], M Ouchabane[1], H Akkari[2], S Hassani[1] and D Dergham[1]

[1] Centre de développement des technologies avancées, Division des Milieux ionisés & Laser, Cité 20 Aout 1956, Baba Hassen, Alger, Algérie
[2] Groupe des matériaux fonctionnels, laboratoire LGMM, Université 20 août 1955—Skikda, route d'El-Hadaiek, B.P : 26, 21000 Skikda, Algérie

E-mail: flekoui@cdta.dz

Keywords: ZnO-Ag films, thermal evaporation, transmittace, nanohardness

Abstract

ZnO-Ag thin layers were prepared by thermal evaporation under vacuum and then subjected to recrystallization annealing heat treatment under atmosphere at 300, 400 and 500 °C to ensure oxidation and crystallization of ZnO. The results showed the evolution of these properties as a function of the annealing temperature. XRD analysis indicate that the crystallization of ZnO increase with annealing temperatures. The same observation was underlined for the transmittance with annealing temperature. However, the samples without annealing and those annealed at 300 and 400 °C appeared to be conductive with a resistance of 1.1 Ω, 0.67 Ω and 2.1 Ω while the sample annealed at 500 °C have a resistance of $1.73.10^5$ Ω which belongs to a semiconductor material. As recognized, the hardness of the deposited layers as a function of the grain size does not respect the Hall-Petch relationship because of the grains size lower than 100 nm.

Introduction

Zinc oxide (ZnO) is a semiconductor material with interesting physical properties that place it among the most promising materials for use in various fields such as piezoelectricity, photovoltaic effect, optoelectronics and gas detection [1–3]. The ZnO crystallizes in a hexagonal Würtzite structure belonging to the $P6_3mc$ space group which is strongly ionic with 3.37 eV of band gap and a high excitons binding energy of 60 MeV at room temperature [4]. The addition to ZnO layers of other metallic elements such as silver (Ag) consists of controlling the physical properties of the layer. Silver is a very important element used as dopant, composite layer or multilayer with ZnO [5–7]. It was widely studied as a major candidate for materials with a broad band gap to absorb light [8]. Moreover silver has theoretically the lowest transition energy and a shallow acceptor level at 0.3 eV above the maximum valence band related to copper and gold [3]. At the two sites Ag tends to occupy the substitutional sites of Zn (Ag_{Zn}) and interstitial (Ag_i) while the energy of formation of Ag_{Zn} is less than Ag_i, which makes Ag as an excellent candidate for p-type doping [9]. The ZnO-Ag layer has proved its importance in the field of surface treatments thanks to its interesting optical, electrical, photocatalytic and antibacterial properties [10, 11]. Indeed, there are several methods for producing these ZnO-Ag layers as for example Pulsed Laser Deposition (PLD) [12], sputtering [13], Chemical vapor deposition CVD [14], spin coatings [15], photochemical metal-organic deposition [16] and Sol-Gel method [17].

In this present work, thin layers of ZnO-Ag (70:30%) were prepared by thermal evaporation under vacuum and then investigated. On the basis of the experimental results, it is confirmed that the presence of Ag as a transition metal plays an important role on the electrical properties of ZnO. The role of the annealing temperature in the crystallization of ZnO and its effect on the morphology, topography, transmittance of the layer is also noted and discussed. The mechanical stability and behavior of zinc oxide under ZnO-Ag alloy and the effect of annealing temperature on hardness and Young's modulus need more investigation since such aspect has not been studied before. The obtained results showed that annealing temperature is a key parameter in modifying and adjusting the elasto-plastic properties of which are of great importance in ZnO-Ag based devices.

Experimental procedures

ZnO-Ag thin films were prepared by the vacuum thermal evaporation method on ordinary glass substrates (Stairway) 1.0 mm thick and 25*75 mm^2 surface with a mass ratio between ZnO and Ag (70:30%). The powder of ZnO and Ag sphere were purchased from SIGMA-ALDRICH and GoodFellow50 with 99% and 99.99% of purity, respectively. Before deposition the substrates were first cleaned with acetone and ethanol solution in an ultrasonic bath and then mounted onto the substrate holder. Even though the melting point of ZnO and Ag are different, the evaporation process was started after pumping the chamber till a residual pressure around 3.10^{-6} mbar. ZnO-Ag films were prepared by heating a mixture of ZnO oxide powder and pure Ag grains in a tungsten crucible with a thermal evaporation process of few seconds. After deposition, in order to improve the material quality the as-deposited samples were annealed under atmospheric pressure at three different temperatures 300, 400 and 500 °C for one hour and then characterized to show possible structural changes induced by ambient oxygen and resulting in different properties.

The structure changes of films were identified by XRD technique, using Philips X'PertMPD diffractometer with a Cu-Kα cathode source and 1.54 Å of wavelength.

The scanning electron microscopy (SEM) imaging of ZnO-Ag thin films was performed using an instrument (SEM, JEOL JSM-6360LV) with an acceleration voltage between 5 kV–15 kV.

The surface roughness was analyzed with the Atomic Force Microscopy (AFM) technique. The AFM tip is of silicone material with a radius of curvature less than 50 nm and a silicon nitride lever. The scanning area is between 1 to 80 μm maximum.

The optical properties were investigated by using a spectrophotometer (OPTI ZEN 3220 UV) in UV-Visible range (200–800 nm) while the electrical properties measurements were carried out by four point probe Keithley's 2400C (200V, 1A, 20W SourceMeter SMU Instrument with contact check) instrument where the measured current is only driven by the layer since the substrate is significantly more insulating than the layer material.

Themechanical properties (E and H) were measured using a Berkovich indenter of CSM testing instrument based on the Oliver-Pharr method. The used Poisson's ratio and the force applied by the indenter are 0.3 and 3.0 mN, respectively. It is worth noting that during the test of nanoindentation on thin films the tip penetration depth is of great importance to avoid the substrate effect when collecting nanoindentation data. To eliminate such effects the penetration depth must not exceeds 1/10 to 1/5 of the film thickness [18]. This established rule was respected during all nanoindentation tests.

Results and discussions

First of all let's see the structure of ZnO evaporated and annealed layers to make possible results comparison with those of ZnO-Ag material. Figure 1 represents the XRD patterns of the as-deposited and annealed ZnO layers at 300, 400 and 500 °C. It appears from XRD peaks that ZnO powder is evaporated and deposited into polycrystalline structure represented by Zn and ZnO phases as identified. The heating process at different temperatures leads to the crystallization of ZnO phase through oxidation by the surrounding oxygen in the atmosphere.

Besides, figure 2 shows the XRD patterns of the as-deposited and annealed thin ZnO-Ag layers at 300, 400 and 500 °C. At first glance, one can see the presence of Ag peaks with preferential direction (111) and ZnO peaks without any preferential direction. However, it appears that the evolution of the oxidation and the crystallization of ZnO-Ag layers are more improved after the annealing treatment where such changes begin to be affected at 300 °C and come clearly noticeable at 500 °C. The intensity of the known diffraction peaks at (100), (002) and (101) belonging to hexagonal wurtzite structure increases slightly with increasing annealing temperature. This means that the structure is randomly oriented and there is no preferential orientation of the structure at such temperatures. Indeed, as described before about the evaporation process and according to L'Vov *et al* [19] the ZnO powder changes from solid to vapor state after heating till evaporation temperature and yields atomic oxygen that is not totally pumped outside the chamber. This is why at room temperature the deposited layer contains a poor quantity of ZnO phase which is formed through Zn oxidation from the adsorbed atomic oxygen on substrate top surface. Here, silver oxide formation is excluded since thermodynamic conditions are not met as claimed by L'Vov [20] and Karunakaran *et al* [21]. Indeed, the adsorbed atomic oxygen is trapped by the subsequent Zn evaporated particles but leads to low ZnO phase concentration obtained from oxidation reaction. However, after thermal annealing of the deposited layers at 300, 400 and 500 °C the structure is remarkably modified by oxygen incorporation given by the atmosphere. As it can be observed from figure 2, the XRD spectra of the annealed samples show that wurtzite structure of ZnO begins to appear in the directions (100), (002), (101) and (102) after annealing at 300 °C. It is clearly apparent that the increase in peak intensity can be explained by

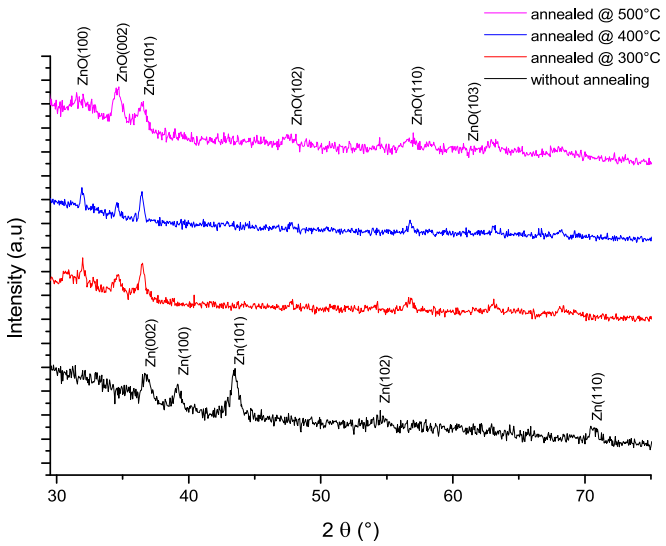

Figure 1. XRD patterns of as-deposited and annealed ZnO layers.

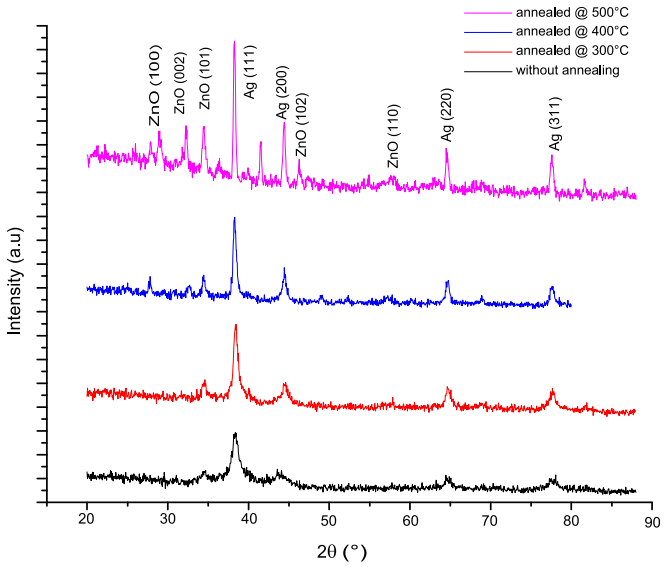

Figure 2. XRD patterns of as-deposited and annealed ZnO-Ag layers.

the increase of more Zn oxidation and well crystallized structure. From XRD patterns one can estimate the grain size from the most intense peak Ag (111) by using the Debye–Scherrer formula [22]:

$$D = (0.9/\beta.\cos\theta).\lambda$$

Where D is the grain size, β, θ and λ are respectively the full width at half maximum, the Bragg diffraction angle and the wavelength of the used x-rays source.

As represented by figure 3, it is found that the Ag particles have their grain size increasing from 12 nm at room temperature to stabilize at a maximum value of 28 nm for annealing temperature settled at 500 °C. This change in grain size appears to be closely related to oxidation rate as the temperature is increased. Therefore, at low temperature the incorporated quantity of oxygen is low resulting in fine microstructure while larger grain sizes are observed at higher temperature. Similar oxidation effect was observed by Jitao Li *et al* [23, 24].

The AFM surface topography of the layers is shown by figure 4 (images 4a, 4b, 4c and 4d). All the layers have a similar topography consisting of more or less identical particles whose size increases with the annealing temperature as we discussed above. The AFM images show that the lowest mean roughness of 54 nm is obtained for layer without annealing while the highest mean value of 186 nm is obtained at annealing temperature of 500 °C (see table 1).

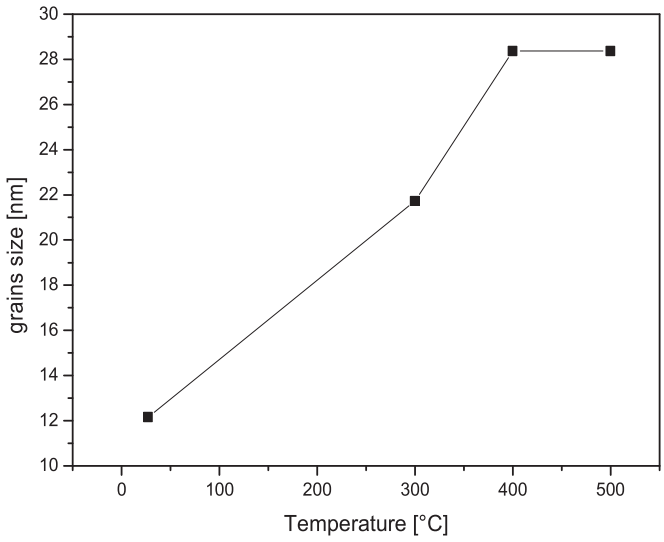

Figure 3. Variation of Ag grain size with annealing temperature.

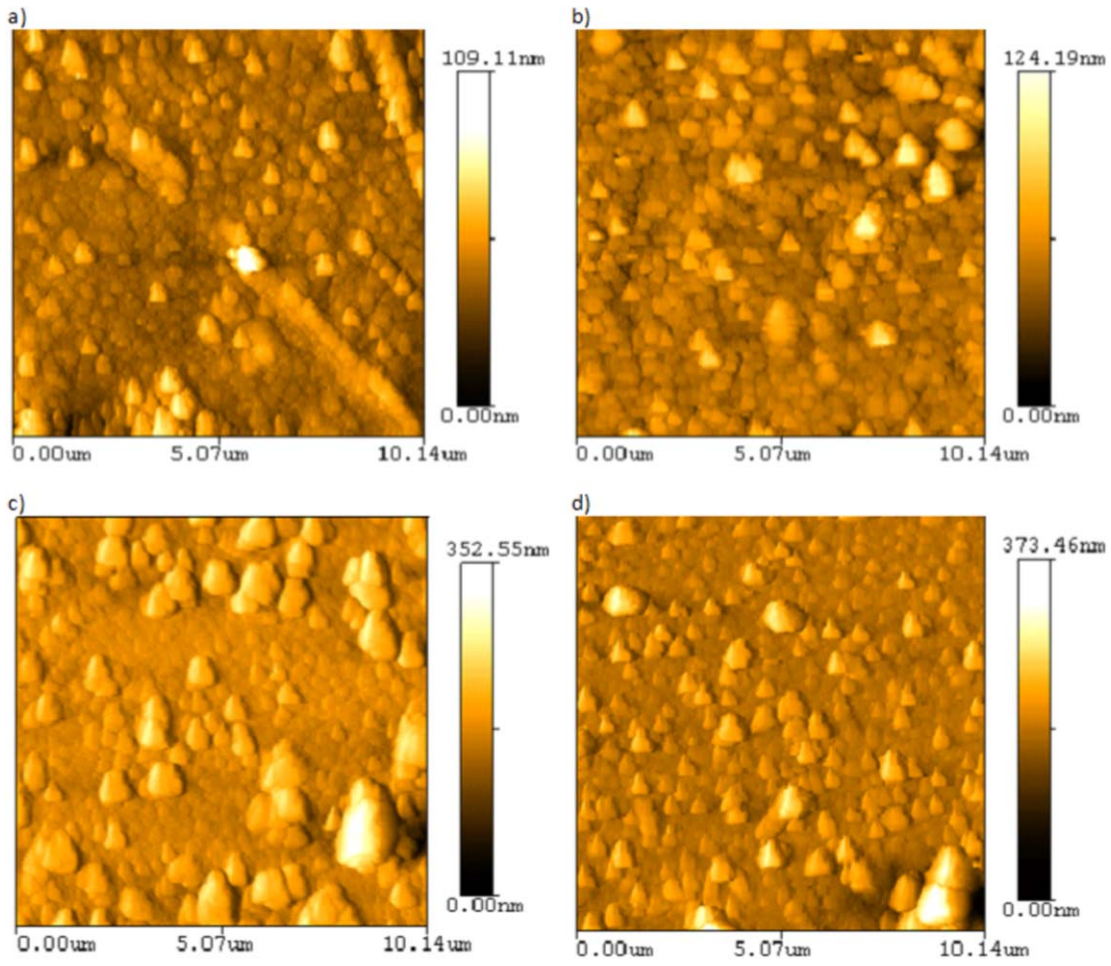

Figure 4. AFM images of surfaces; without annealing (a) and annealed at 300 °C (b), 400 °C (c) and 500 °C (d).

This increase in surface roughness is probably due to the formation and agglomeration of ZnO nanocrystallite. This is promoted by oxidation of thermally activated particles with high mobility in the lattice which tends to agglomerate and stabilize as larger particles in size as reported by Yang *et al* [25].

Table 1. Values of roughness, transmittance and resistance of ZnO-Ag layers.

	Without annealing	Annealing@300 °C	Annealing@400 °C	Annealing@500 °C
Roughness [nm]	54	63	177	186
Transmittance [%]	24	40	50	80
Resistance [Ω]	1.1	0.67	2.1	$1.73\ 10^5$

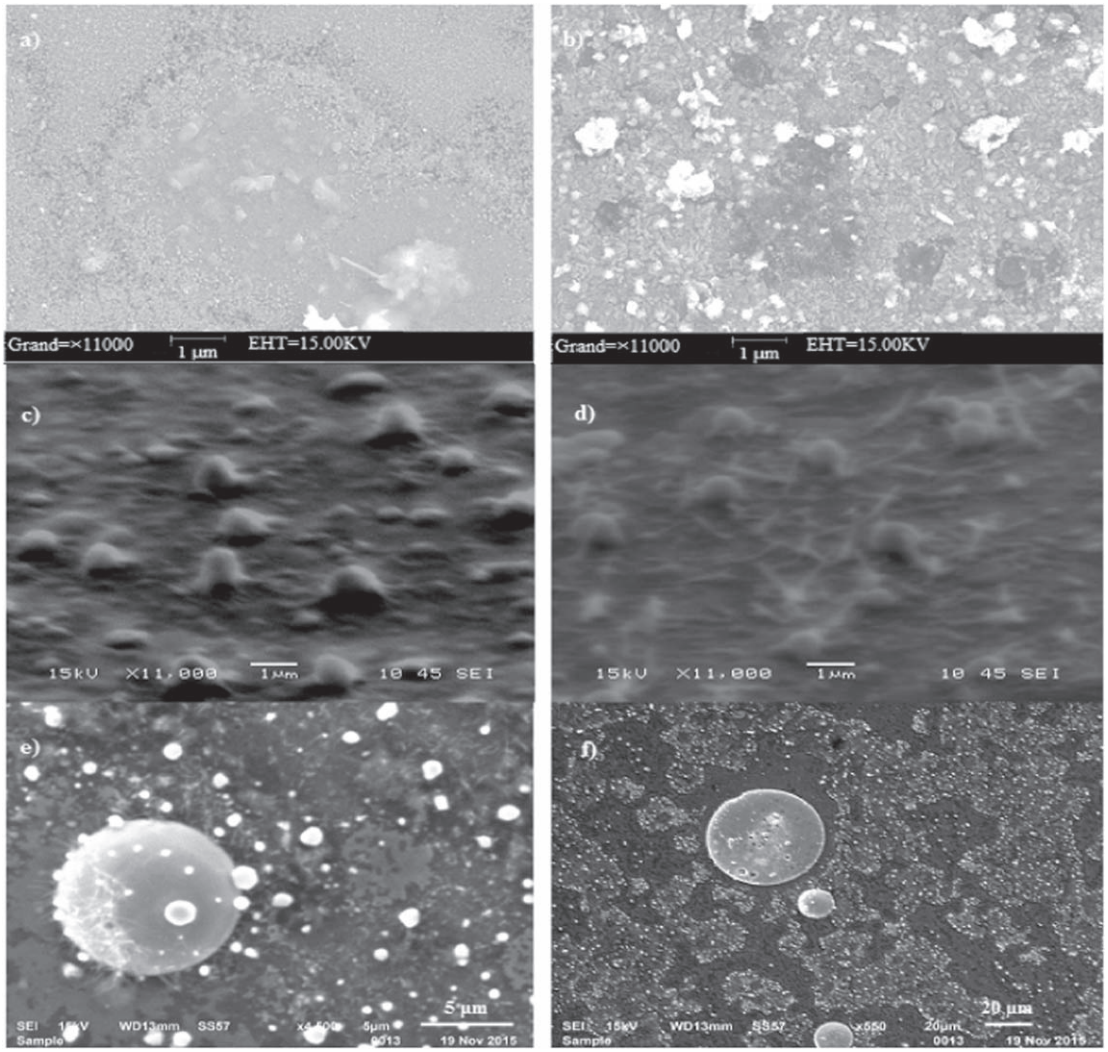

Figure 5. SEM images of the surfaces; without annealing (a) annealed at 300 °C (b), 400 °C (c), 500 °C (d), and (e), (f) : images of Ag agglomeration at 500 °C with 4500 and 550 magnification respectively.

Figures 5(a)–(f) taken by scanning electron microscopy show morphological aspects of ZnO-Ag layers on top surface as a function of annealing temperature. As we can see the top surface morphology is remarkably affected by annealing temperature and oxidation. Here, the selected temperature has a twice effect; it increases the atomic mobility of the network and making easier oxygen incorporation to form ZnO crystals. The as-deposited layer without annealing temperature is smooth with some irregular shaped particles spread out over the surface while it becomes rough as the layer is annealed At 300 °C (figure 5(b)), it appears clearly that the deposited particles change in shape and multiply as shown by AFM technique. Moreover, at 400 °C of annealing temperature microrod pillar can be observed at early growth stage embedded in the matrix (figure 5(c)) while at 500 °C (figures 5(d)–(f)) spherical microparticles appear on the whole surface and surrounded by a nanowire-like structure. This obtained microstructure at such temperatures can be explained by Ag particles that have a tendency to agglomerate as island-like or spherical particles as investigated by Cheng *et al* [26] and as it appears in figure 5(f) where spherical shape agglomerated particles dispersed on top surface confirms this statement.

For more insight on the annealing effect on the properties of the deposited films spectrophotometric electrical and nanoindentation measurements were performed on the ZnO-Ag layers. Figure 6 displays the

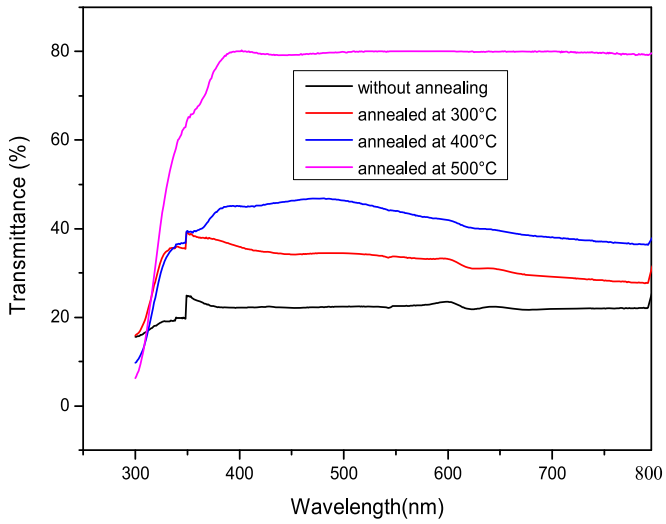

Figure 6. Transmission spectra of the ZnO-Ag layer with various annealing temperatures.

optical transmittance spectra in the range of 300–800 nm. It is clearly apparent that the maximum (80%) of transmission is obtained at 500 °C of annealing temperature while transmissions equal or less than 50% were obtained for the as-deposited ZnO-Ag layers and annealed at 300 °C and 400 °C. This optical behavior as a function of annealing temperature can be inferred to the microstructural changes discussed above and enhanced by the presence of Ag particles. It is demonstrated [27] that optical properties of ZnO-Ag layers are governed by metallic particles through exhibiting a surface plasmon resonance (SPR) with characteristics that are dependent on the size, shape and orientation of those particles as well as the refractive index of the matrix. Indeed, our above explanation on surface diffusion and agglomeration of Ag particles affect their size and shape and then strengthen the finding reported by Johnson and Christy [28]. Thus, the high transmission at 500 °C can be explained by the diffusion and agglomeration of the Ag particles which leads to a larger surface of the ZnO phase and hence allows transmitting more light intensity through the ZnO phase which is known to be transparent in this range.

The respective determined electrical resistance values are 1.1 Ω, 0.67 Ω and 2.1 Ω show that the as-deposited ZnO-Ag layer is conductive as well as those annealed at 300 °C and 400 °C. However, what is noticeable is the jump of the electrical properties from conductive to semiconductor layer at annealing temperature of 500 °C. This confirms that Ag particles play a key role in tuning the electrical conductivity of ZnO-Ag layers and by diffusion enhanced temperature the Ag particles agglomerate making less surface equivalent conductivity with difficult current conduction within the material. As a result, the measured value of 1.73 10^5 Ω expresses more the electrical properties of ZnO material.

Figure 7 shows the diagrams of the hardness evolution as a function of the annealing temperature. The results show that the grain size as well as the hardness of the layer increase with increasing annealing temperature. This tendency appears to be understandable since the annealing temperature improves the degree of crystallinity of the layers which makes them with more density and then more hardness. However, what is surprising is that such a result does not respect the known Hall-Petch formula that expresses the relationship between mechanical properties and grain size; hardness evolves in the same way as grain size. Besides, other authors [29–32] make this relationship as a function of different parameters such as grain size, surface morphology and topography, crystallographic orientations, film density, lattice parameters and stoichiometry.

Indeed, the indentation test is a deformation of certain amount of a material where the elasto-plastic properties are governed by the creation and propagation of dislocations during the loading and unloading process with polycrystalline materials, though not limited to the only one, the grain size is a key parameter in determining the mechanical properties where the grain boundaries represent an effective barrier to the dislocation propagation. However, when the grain sizes are in the nanometer range (<100 nm) the dislocation theory for the Hall-Petch effect is not respected but can be explained by many theoretical models based on different deformation mechanisms as confirmed by Pande and Masumura [33]. Such an outcome eliminates any uncertainty of our results about the nanomechanics of Hall-Petch relationship in ZnO-Ag material with grains of nanometer scale. Thus, the straight forward assumption that can be relied upon in the interpretation of these results is the lattice dislocation slip model used for nanocrystalline materials. The model takes into account a smaller grain size with a high density of grain boundary with the condition that the lattice dislocation motion occurs within grains containing low dislocation density. Therefore, under such conditions the inverse Hall-

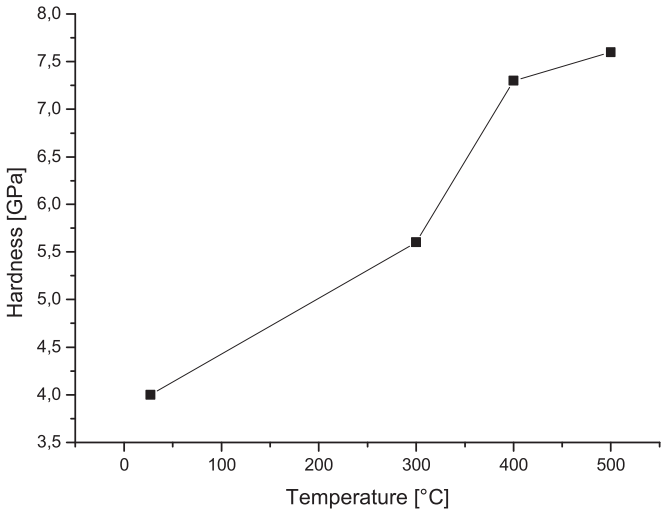

Figure 7. Variation of Hardness with annealing temperature.

Table 2. Values of hardness, Young's modulus, H/E,H^3/E^2 and E^2/H.

	As-deposited	@300 °C	@400 °C	@500°C
H [GPa]	4	5, 6	7, 3	7, 6
E [GPa]	90	70	80	115, 4
H/E	0, 04	0, 08	0, 09	0, 06
H^3/E^2	0, 008	0, 03	0, 06	0, 03
E^2/H	2025	875	876, 7	1752, 2

Petch effect explains well our results as proposed by Pande and Masumura due to the non-proportionality between the length of pile-up and the number of dislocation and also by the fact that the grain boundaries act as a sink for dislocations as suggested by Malygin [34].

Additionally, the elasto-plastic properties of the deposited ZnO-Ag layers are expressed in terms of H/E, H^3/E^2 and E^2/H and the results are summarized in table 2.

From this table, one can observe that the elasto-plastic behaviors of the thin layers are not the same as a function of temperature. It is recognized [35] that the smaller value of H/E means that the material exhibits much smaller elastic strains that the plastic ones such as the as-deposited ZnO-Ag thin film. The increase rate of elasticity in case of annealed samples is due to Ag agglomeration which leaves more possibilities to ZnO crystallization. On the other side, the measured values of H^3/E^2 ratio, which is defined as the plastic resistance parameter [36] reveal that the contact load needed to induce plastic deformation is low for the as-deposited ZnO-Ag material. On the other hand, E^2/H as an indication of the material's resistance to plastic indentation [37] show that for a given hardness (sample @ 400 °C and sample @ 500 °C) the parameter E^2/H gives different values indicating that the material with lower elastic modulus accommodate more and has the better resistance to permanent damage when the indenter is removed as confirmed by Joslin and Pharr [37].

Conclusion

ZnO-Ag thin layers were produced by thermal evaporation under vacuum and subjected to different annealing temperatures under atmospheric conditions. It has been found that the crystallinity, grain size and roughness of layers increase with annealing temperature. It is found that the annealing temperature has a great effect on the transparency of the deposited layers in the visible range; it increases with annealing temperature. ZnO-Ag layers with high transparency (80%) were obtained at 500 °C of annealing temperature. The electrical properties are also influenced by annealing temperature that leads to both conductive and semi-conductive layers. The measured hardness showed an increasing behavior with annealing temperature which is a reverse behavior to Hall-Petch law. Evaluation of elasto-plastic properties in terms of H/E, H^3/E^2 and E^2/H allows us to conclude that on the possibility to synthesize materials with different hardness and Young's modulus but with the same elasto-plastic behaviors.

Acknowledgments

We are grateful for Prof Francisco de Paula Martín Jiménez, from university of Malaga (Spain) for his assistance during XRD data collection. Grateful are also addressed to Université Ferhat Abbas-Sétif for doing AFM measurements.

ORCID iDs

F Lekoui https://orcid.org/0000-0003-4649-1290

References

[1] Pogrebnjak A D, Jamil N Y and Muhammed A K M 2011 Structural, optical properties of ZnO prepared by CVD before and after annealing *Metallofiz Noveishie Tekhnol.* **33** 235–41
[2] Kim Y S, Tai W P and Shu S J 2005 Effect of preheating temperature on structural and optical properties of ZnO thin films by sol–gel process *Thin Solid Films* **491** 54–60
[3] Deng R and Tang Y Z H 2008 Correlation between electrical, optical properties and Ag^{2+}centers of ZnO:Ag thin films *Physica B: Condensed Matter* **403** 2004–7
[4] Teke A, Zgür Ü Ö, Dogan S, Gu X H, Morkoc H, Nemeth B, Nause J and Everitt H O 2004 Excitonic fine structure and recombination dynamics in single-crystalline ZnO *Phys. Rev.* B **70** 195207
[5] Azizi S, AhmadB M, Hussein M Z and Ibrahim N A 2013 Synthesis, antibacterial and thermal studies of cellulose nanocrystal stabilized ZnO-Ag heterostructure nanoparticles *Molecules.* **18** 6269–80
[6] Lin D, Wu H, Zhang R and Pan W 2009 Enhanced photocatalysis of electrospun Ag−ZnO heterostructured nanofibers *Chem. Mater.* **21** 3479–84
[7] Karunakaran C, Rajeswari V and Gomathisankar P 2011 Enhanced photocatalytic and antibacterial activities of sol–gel synthesized ZnO and Ag-ZnO *Materials Science in Semiconductor Processing* **14** 133–8
[8] Amornpitoksuk P, Suwanboon S, Sangkanu S, Sukhoom A, Muensit N and Baltrusaitis J 2012 Synthesis, characterization, photocatalytic and antibacterial activities of Ag-doped ZnO powders modified with a diblock copolymer *Powder Technol.* **219** 158–64
[9] Chen R, Zou C, Bian J, Sandhu A and Gao W 2011 Microstructure and optical properties of Ag-doped ZnO nanostructures prepared by a wet oxidation doping process *Nanotechnology* **22** 105706
[10] Jamil N Y, Najim S A, Muhammed A M and Rogoz V M 2014 Preparation, structural and optical characterization of ZnO/Ag thin film by CVD *Proc. of the international conference nanomaterials: Applications and properties* 302NEA09
[11] Punith Kumar M K and Srivastava C 2013 Morphological and electrochemical characterization of electrodeposited Zn–Ag nanoparticle composite coatings *Material Characterization* **85** 82–91
[12] Kang K-M, Choi Y-J, Kim H and Park H-H 2015 Structural, electrical and optical properties of photochemical metal-organic-deposited ZnO thin films incorporated with Ag nanoparticles and graphene *ECS Journal of Solid State Science and Technology* **4** 55–9
[13] Francq R, Snyders R and Cormier P A 2017 Structural and morphological study of ZnO-Ag thin films synthesized by reactive magnetron co-sputtering *Vaccum* **137** 1–7
[14] Wenas W W, Yamada A, Takahashi K, Yoshino M and Konagai M 1991 Electrical and optical properties of boron-doped ZnO thin films for solar cells grown by metalorganic chemical vapor deposition *J. Appl. Phys.* **70** 7119–23
[15] Lin S-L, Hsu K-C, Hsu C-H and Chen D-H 2013 Hydrogen treatment-improved uniform deposition of Ag nanoparticles on ZnO nanorod arrays and their visible-light photocatalytic and surface-enhanced Raman scattering properties *Nanoscale Res. Lett.* **8** 325
[16] Kryshtab T, Khomchenko V S, Khachatryan V B, Roshchina N N, Andraca-Adame J A, Lytvyn O S and Kushnirenko V I 2007 Effect of doping on properties of Zno:Cu and Zno:Ag thin films *J. Mater. Sci., Mater. Electron.* **18** 1115–8
[17] Chelouche A, Djouadi D, Merzouk H and Aksas A 2014 Influence of Ag doping on structural and optical properties of ZnO thin films synthesized by the sol-gel technique *Appl. Phys.* A **115** 613–6
[18] Zhao M, Xiang Y, Xu J, Ogasawara N, Chiba N and Chen X 2008 Determining mechanical properties of thin films from the loading curve of nanoindentation testing *Thin Solid Films* **516** 7571–80
[19] L'vov B V, Ugolkov V L and Grekov F F 2004 Kinetics and mechanism of free-surface vaporization of zinc, cadmium and mercury oxides analyzed thermogravimetrically by the third-law method *Thermochim Acta.* **411** 187–93
[20] L'vov B V 2001 The physical approach to the interpretation of the kinetics and mechanisms of thermal decomposition of solids: the state of the art *Thermochimica Acta.* **373** 97–124
[21] Karunakaran C, Rajeswari V and Gomathisankar P 2011 Optical, electrical, photocatalytic, and bactericidal properties of microwave synthesized nanocrystalline Ag-ZnO and ZnO *Solid States Sciences.* **13** 923–8
[22] Li J, Yang D, Zhu X, Sun H, Gao X, Wangyang P and Tian H 2017 Structural and optical properties of nano-crystalline ZnO thin films synthesized by sol–gel method *J Sol-Gel SciTechnol.* **82** 563–8
[23] Li J, Yang D and Zhu X 2017 Effects of aging time and annealing temperature on structural and optical properties of sol-gel ZnO thin films *AIP Adv.* **7** 065213
[24] Li J, Yang D and Zhu X 2017 Pretreating temperature controls on structural, morphological and optical properties of sol–gel ZnO thin films *Mater. Technol.* **33** 198–204
[25] Yang L, Duponchel B, Cousin R, Gennequin C, Leroy G, Gest J and Carru J C 2012 Structure, morphology and electrical characterizations of direct current sputtered ZnO thin films *Thin Solid Films* **520** 4712–6
[26] Cheng P, Li D, Yuan Z, Chen P and Yang D 2008 Enhancement of ZnO light emission via coupling with localized surface plasmon of Ag island film *Appl. Phys. Lett.* **92** 041119
[27] Mohammed HosseinHabibiandRezaSheibani 2010 Preparation and characterization of nanocomposite ZnO–Ag thin film containing nano-sized Ag particles: influence of preheating, annealing temperature and silver content on characteristics *J Sol-Gel SciTechnol.* **54** 195–202
[28] Johnson P B and Christy R W 1972 Optical constants of the noble metals *Phys. Rev.* B **6** 4370–4279
[29] Khojier K and Savaloni M R K M H 2013 Annealing temperature effect on the mechanical and tribological properties of molybdenum nitride thin films *Journal of Nanostructure in Chemistry* **3** 5

[30] Hainsworth S V and Soh W C 2003 The effect of the substrate on the mechanical properties of TiN coatings *Sur. Coat. Technol.* **163–164** 515–20
[31] Patsalas P, Charitidis C and Logothetidis S 2000 The effect of substrate temperature and biasing on the mechanical properties and structure of sputtered titanium nitride thin films *Sur. Coat. Tech.* **125** 335–40
[32] Harlin P, Carlsson P, Bexell U and Olsson M 2006 Influence of surface roughness of PVD coatings on tribological performance in sliding contacts *Surf.Coat.Technol.* **201** 4253–9
[33] Pande C S and Masumura R A 1996 *Processing and Properties of Nanocrystalline Materials* ed C Suryanarayana *et al* (Warrendale, PA: TMS) vol 387
[34] Malygin G A 1995 Break-down of the Hall-Petch law in micro and nanocrystalline materials *Phys Solid State* **37** 1248–53
[35] Giannakopoulos A E and Zisis T H 2011 Analysis of Knoop indentation strain hardening effects *Int. J. Solids Struct.* **48** 175–90
[36] Tsui T Y, Pharr G M, Oliver W C, Bhatia C S, White R L, Anderst S, Andersi A and Brownt I G 1995 Nanoindentation and nanoscratching of hard carbon coatings for magnetic disks *Mat. Res. Soc. Symp. Proc.* **383** 447–52
[37] Joslina D L and Oliver W C 1990 A new method for analyzing data from continuous depth-sensing microindentation tests *J. Mater. Res.* **5** 123–6